Decentralized Charging Coordination of Electric Vehicles under Feeder Capacity Constraints

Juan Martinez-Piazuelo, Nicanor Quijano, *Senior Member IEEE*,
Carlos Ocampo-Martinez, *Senior Member IEEE*

***Abstract*— As an envisioned technology for future smart city networks, this paper studies the real-time decentralized charging coordination of a fleet of plug-in electric vehicles (PEVs) under feeder capacity constraints. In particular, inspired by some ideas in the field of population games and payoff dynamics models, we propose a novel form of continuous-time primal-dual gradient dynamics and develop a real-time control method for the charging coordination of PEVs in smart city networks. The proposed method is able to coordinate the charging profiles of multiple PEVs in a decentralized fashion under a general convex optimization objective, and guarantees the satisfaction of the operational constraints of the PEVs and the feeder lines of the distribution network for all times. The optimality and asymptotic stability of the proposed dynamics are formally proven, and the advantages of the proposed method are illustrated through numerical simulations considering a fleet with several PEVs.**

I. Introduction

Through the integration of multiple novel technologies, future smart cities are expected to play a crucial role in the mitigation of the environmental footprint of the modern industry. Namely, one of the most envisioned of such novel technologies are plug-in electric vehicles (PEVs). For instance, by fostering a high penetration of PEVs, future smart cities could not only provide low emission transportation systems, but might also bring power flexibility to support green energy generation services [1], [2], [3], [4]. However, since the uncoordinated charging of multiple PEVs can lead to power losses and overloads on the transformers and feeders of the distribution network [5], [6], [7], having a high penetration of PEVs imposes some significant challenges as well. Hence, the future smart cities should provide mechanisms to coordinate the charging process of their PEVs, not only to better integrate sustainable energy resources, but also to ensure the safe operation and economic efficiency of the electrical grid.

Juan Martinez-Piazuelo and Nicanor Quijano are with the Department of Electrical and Electronics Engineering at Universidad de los Andes, Bogotá, Colombia. Juan Martinez-Piazuelo and Carlos Ocampo-Martinez are with the Automatic Control Department at Universitat Politécnica de Catalunya, Barcelona, Spain. Corresponding author: Juan Martinez-Piazuelo (juan.pablo.martinez.piazuelo@upc.edu).

Juan Martinez-Piazuelo gratefully acknowledges the Universitat Politècnica de Catalunya and Banco Santander for the financial support of his predoctoral grant FPI-UPC. In addition, the authors would like to thank the project PID2020-115905RB-C21 (L-BEST) funded by MCIN/ AEI /10.13039/501100011033 for supporting this research. Finally, Nicanor Quijano would like to thank the UK-PACT Project (2019-2021), Systemic perspectives on low-carbon cities in Colombia – An integrated urban modelling approach for policy and regulatory analysis.

Recently, several works have addressed the decentralized charging coordination of PEV fleets [8]. One popular approach, investigated in [9], [10], [11], [12], employs a two-stage iterative process that operates as follows. On the first stage, each PEV solves a local optimization problem considering a common electricity price signal, and communicates its resulting charging schedule to an aggregator node. On the second stage, the aggregator node updates the price signal based on the PEVs responses, and broadcasts the updated signal to the PEVs. The two stages are repeated until convergence of the price signal. Once the iterative process ends, the PEVs proceed to execute their computed charging schedules. Although this approach usually converges to an optimal charging coordination profile, the practical implementation of the method might suffer from the uncertainty associated to the arrival and departure times of the PEVs. Notice that if some PEVs arrive or leave after the optimal profile has been computed, then the entire iterative process has to be repeated. Moreover, the algorithms in [9], [10], [11], [12] do not consider coupled constraints over the PEVs, e.g., the capacities of the feeder lines of the distribution network, and it remains unclear how to properly include such constraints within the proposed methods. On the other hand, the author in [13] proposes a continuous-time feedback (gradient-type) control law to fill the overnight demand valley under uncertainties. Although the proposed approach can deal with arrival and departure times uncertainties, it does not consider coupled constraints over the PEVs. Similarly, the authors in [14] propose an iterative water-filling method, but again, the method does not consider coupled constraints and the aggregator needs to perform sequential computations that might not properly scale for large populations of PEVs. In contrast, the authors in [15] and [16] propose a gradient projection method and a primal-dual subgradient method, respectively, to deal with the feeder capacity constraints of the distribution network. Nevertheless, the proposed approaches only guarantee the satisfaction of the feeder capacity constraints at the convergence of the algorithms, and, thus, may not be applicable under a real-time control scheme that could deal with the uncertainties of the arrival and departure times of the PEVs, while also satisfying the hard operational constraints of the system.

Motivated by the approaches in [13] and [16], in this paper we propose a real-time optimization-based control method to coordinate the charging process of a fleet of PEVs under coupled feeder capacity constraints. The core of our method is the development of a novel form of continuous-time primal-dual gradient dynamics [17], which are inspired on the ideas of population games and payoff dynamics models [18], [19], [20], [21]. Note that various continuous-time primal-dual gradient dynamics have been proposed for other network and power grid related applications [22], [23], [24]. However, the dynamics proposed in this paper have certain invariance properties that make them attractive for the PEVs charging coordination task.

In summary, our proposed approach has the following novelties. In contrast with the approaches in [9], [10], [11], [12], [13], [14], our method considers feeder capacity constraints that couple the PEVs' charging schedules. Moreover, in contrast with [15] and [16], our approach satisfies the operational constraints of the system for all times and thus is applicable in real time (i.e., when operating under hard constraints, the PEVs do not have to wait until convergence to apply their corresponding charging profiles). Such a property of the algorithm is especially attractive to respond, in the sense of disturbance rejection, to uncertain arrivals and departures of the PEVs. Finally, in contrast with the primal-dual method in [16], our method does not require repeated hyperplane projections to satisfy the charging constraints of the PEVs, and, hence, reduces the computational load of the PEVs. This is due to the invariance properties of our proposed dynamics, which do not hold under other primal-dual gradient dynamics as the ones in [22], [23], [24], [17]. It is also worth to highlight that in our previous publication [25], we have considered a charging coordination scenario similar to the one studied in this paper. However, the dynamics proposed here not only are fundamentally different than the ones in [25], but also consider more general convex optimization objectives (not only convex-quadratic) and allow more general architectures for the power distribution network.

Consequently, the main technical contributions of this paper are fourfold. First, we formulate a novel form of continuous-time primal-dual optimization dynamics and develop a real-time decentralized charging coordination method that considers capacity-constrained feeder lines. Second, we show that the invariance properties of the proposed dynamics guarantee the satisfaction of the PEVs' charging constraints for all times. Third, we prove that the equilibria set of the proposed dynamics is aligned with the solutions of the charging coordination problem. Finally, we prove that the equilibria set of the proposed primal-dual dynamics is asymptotically stable and, therefore, the dynamics can indeed be applied to solve the charging coordination task. In addition, all of our theoretical developments are validated through numerical simulations.

The remainder of this paper is organized as follows. In Section II we state the charging coordination problem that is considered in this paper. Then, in Section III we present our proposed real-time control method and the corresponding continuous-time primal-dual gradient dynamics. Afterwards, in Section IV we establish our main theoretical results regarding the proposed continuous-time optimization dynamics. Finally, in Section V we present some illustrative numerical simulations, and in Section VI we provide some concluding remarks and future directions of research. Additionally, all the proofs of our theoretical developments are provided in the Appendix.

II. Problem Statement

Consider a set of $n_{\mathcal{V}} \in \mathbb{Z}_{\geq 1}$ PEVs, $\mathcal{V} = \{1, 2, \ldots, n_{\mathcal{V}}\}$, which seeks to coordinate their charging profiles over a multi-time period $\mathcal{T}$. Let $\mathcal{T}^i = \{1, 2, \ldots, n_{\mathcal{T}^i}\}$, with $n_{\mathcal{T}^i} \in \mathbb{Z}_{\geq 1}$, be the charging period of the i-th PEV, so that the multi-time period $\mathcal{T}$ is constructed as $\mathcal{T} = \cup_{i \in \mathcal{V}} \mathcal{T}^i = \{1, 2, \ldots, \max_{i \in \mathcal{V}} n_{\mathcal{T}^i}\}$. Here, 1 denotes the present time slot, 2 the next one, and so on. Throughout, we assume that all the time slots within $\mathcal{T}$ have the same duration $\delta \in \mathbb{R}_{>0}$ (with units of hours). Moreover, let $\mathcal{V}_k \subseteq \mathcal{V}$ be the set of PEVs that have the k-th time slot within their charging period, i.e., $\mathcal{V}_k = \{i \in \mathcal{V} : k \in \mathcal{T}^i\}$, for all $k \in \mathcal{T}$. Finally, to ease the forthcoming discussions, let $\mathcal{T}_e^i = \mathcal{T}^i \cup \{0\}$ be the extended set of charging time slots of the i-th PEV, which includes a fictitious charging time slot denoted by 0 that is used to allocate the excess of power.

Under the considered framework, for each PEV $i \in \mathcal{V}$ the charging power that is scheduled to be injected at the time slot $k \in \mathcal{T}_e^i$ is denoted by $x_k^i \in \mathbb{R}_{\geq 0}$ (with units of kW). Therefore, the scheduled charging profile of the i-th PEV is given by the vector $\mathbf{x}^i = \left[x_0^i, x_1^i, x_2^i, \ldots, x_{n_{\mathcal{T}^i}}^i\right]^\top \in \mathbb{R}_{\geq 0}^{(n_{\mathcal{T}^i}+1)}$, where x_0^i is a fictitious charging power for all $i \in \mathcal{V}$, and the collection of the scheduled charging profiles of all the PEVs is given by $\mathbf{x} = \left[\left(\mathbf{x}^1\right)^\top, \left(\mathbf{x}^2\right)^\top, \cdots, \left(\mathbf{x}^{n_{\mathcal{V}}}\right)^\top\right]^\top \in \mathbb{R}_{\geq 0}^n$, where $n = \sum_{i \in \mathcal{V}} (n_{\mathcal{T}^i} + 1)$. Throughout, we consider that a collection of scheduled charging profiles $\mathbf{x}$ is feasible if and only if it satisfies the constraints

$$x_k^i \geq 0, \quad \forall k \in \mathcal{T}_e^i, \quad \forall i \in \mathcal{V}, \tag{1a}$$

$$x_k^i \leq d^i, \quad \forall k \in \mathcal{T}^i, \quad \forall i \in \mathcal{V}, \tag{1b}$$

$$x_0^i + \sum_{k \in \mathcal{T}^i} x_k^i = \frac{e^i(0)}{\eta^i \delta}, \quad \forall i \in \mathcal{V}, \tag{1c}$$

$$\sum_{i \in \mathcal{V}_k} \psi^{z,i} x_k^i \leq c_k^z, \quad \forall k \in \mathcal{T}, \quad \forall z \in \mathcal{F}. \tag{1d}$$

Here, the constraints in (1a) require for the scheduled charging powers to be non-negative; the constraints in (1b) require for the scheduled charging powers to be not greater than the maximum charging rate $d^i \in \mathbb{R}_{>0}$ (with units of kW) of the i-th PEV; the constraints in (1c) require for the scheduled charging powers to avoid overcharging the battery of the i-th PEV, where $e^i(0) \in \mathbb{R}_{\geq 0}$ is the remaining energy capacity (with units of kWh) of the battery of the i-th PEV at the beginning of the present time slot 1, and $\eta^i \in (0, 1]$ is the charging efficiency of the i-th PEV; and, finally, the constraints in (1d) require for the fleet of PEVs to satisfy the capacity constraints of the feeder lines of the distribution network. Regarding the constraints in (1d), $\mathcal{F} = \{1, 2, \ldots, n_{\mathcal{F}}\}$ denotes the set of feeder lines of the distribution network (with $n_{\mathcal{F}} \in \mathbb{Z}_{\geq 1}$); $c_k^z \in \mathbb{R}_{>0}$ is the maximum capacity of the feeder line $z \in \mathcal{F}$ at the time slot $k \in \mathcal{T}$ (with units of kW); and $\psi^{z,i} = 1$ if the PEV $i \in \mathcal{V}_k$ is fed by the feeder line $z \in \mathcal{F}$, and $\psi^{z,i} = 0$ otherwise. Throughout, it is assumed that the i-th PEVs knows its feeder dependency value $\psi^{z,i}$ for all $z \in \mathcal{F}$. Notice that while (1a), (1b), and (1c) regard individual PEV-level decoupled constraints, (1d) considers distribution network-level coupled constraints. In particular, the parameters d^i, $e^i(0)$, and η^i might depend on the characteristics of the charging port, the vehicle type, and the driving style of each PEV, whilst the parameters $\psi^{z,i}$ and c_k^z might depend on the topology and operational constraints of the distribution network. Moreover, observe that (1a) and (1c) imply that $\eta^i \delta \sum_{k \in \mathcal{T}^i} x_k^i \leq e^i(0)$, for all $i \in \mathcal{V}$. Hence, the (non-fictitious) scheduled charging energy to the i-th PEV must not exceed its corresponding remaining energy capacity $e^i(0)$. It is straightforward to verify that under the considered framework, and due to the consideration of the fictitious charging powers x_0^i in (1c), the set of feasible collections of scheduled charging profiles is nonempty.

Remark 1: For every $d^i \in \mathbb{R}_{>0}$, $e^i \in \mathbb{R}_{\geq 0}$, $\eta^i \in (0, 1]$, $\delta \in \mathbb{R}_{>0}$, and $c_k^z \in \mathbb{R}_{>0}$, the set of feasible collections of scheduled charging profiles, $\mathcal{X} = \{\mathbf{x} \in \mathbb{R}^n : \mathbf{x} \text{ satisfies (1)}\}$, is nonempty. In fact, the relative interior of $\mathcal{X}$ is nonempty as well. That is, there exists some $\hat{\mathbf{x}} \in \mathcal{X}$ such that the inequality constraints in (1a), (1b), and (1d), do not bind at $\hat{\mathbf{x}}$. □

Considering the aforementioned constraints, the charging coordination task can be stated as the constrained optimization problem given by

$$\min_{\mathbf{x} \in \mathbb{R}^n} \; J(\mathbf{x}), \quad \text{s.t.} \quad \mathbf{x} \in \mathcal{X}, \tag{2}$$

where $J : \mathbb{R}^n \to \mathbb{R}$ is a cost function that captures the charging coordination objective of the PEVs and/or the electricity provider. For instance, the cost function $J(\cdot)$ might consider both the total energy generation cost as well as some local costs related to the battery degradation of each PEV [9], [10], [11], [12]. Throughout, we assume that $J(\cdot)$ satisfies the following conditions.

Standing Assumption 1: The cost function $J(\cdot)$ is convex and twice continuously differentiable. □

Standing Assumption 2: For all $i \in \mathcal{V}$ and all $k \in \mathcal{T}_e^i$, the partial derivative $\partial J(\cdot)/\partial x_k^i$ can be evaluated using the local information available at the i-th PEV, i.e., each PEV $i \in \mathcal{V}$ knows the functional form of $\partial J(\cdot)/\partial x_k^i$ and has enough local information to evaluate $\partial J(\mathbf{x})/\partial x_k^i$, for all $k \in \mathcal{T}_e^i$. □

Granted that the goal is to develop a decentralized charging coordination algorithm, we assume that each PEV $i \in \mathcal{V}$ computes its own scheduled charging profile $\mathbf{x}^i$ using only local information available at the i-th PEV. Such local information comprises both individual information of the corresponding PEV (e.g., battery level, charging period, battery degradation parameters, maximum charging rate, charging efficiency, and feeder dependency values $\psi^{z,i}$), as well as global aggregated variables sent to the fleet of PEVs by an aggregator node (e.g., aggregated scheduled charging profiles and distribution network-level variables). More formally, we consider the following assumption.

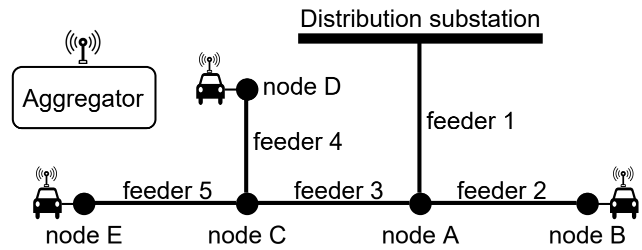

Fig. 1. Distribution network with 5 feeder lines and 3 charging nodes.

Standing Assumption 3: There is an aggregator node that communicates with all the PEVs. The aggregator node is able to receive the scheduled charging profile of each PEV, and is able to send the aggregated scheduled charging profile (i.e., $\sum_{i \in \mathcal{V}_k} x_k^i$, for all $k \in \mathcal{T}$) and distribution network-level variables to the fleet of PEVs. Moreover, the aggregator has full information regarding the feeder dependency values $\psi^{z,i}$, for all $i \in \mathcal{V}$ and all $z \in \mathcal{F}$. □

To ease the exposition of the presented framework, let us introduce some illustrative examples. In particular, Example 1 illustrates the constraints in (1d), and Example 2 provides some optimization objectives that satisfy Standing Assumptions 1 and 2.

Example 1 (Distribution network constraints): Consider the distribution network of Fig. 1. Without loss of generality, assume that there are only three PEVs to be charged (one at node B $\to$ 1, one at node D $\to$ 2, and one at node E $\to$ 3). Thus, $\mathcal{V} = \{1, 2, 3\}$ and $\mathcal{F} = \{1, 2, 3, 4, 5\}$. Moreover, suppose that $\mathcal{T}^1 = \{1\}$, $\mathcal{T}^2 = \{1, 2\}$, and $\mathcal{T}^3 = \{1, 2, 3\}$. Hence, $\mathcal{T} = \{1, 2, 3\}$, $\mathcal{V}_1 = \{1, 2, 3\}$, $\mathcal{V}_2 = \{2, 3\}$, and $\mathcal{V}_3 = \{3\}$. Under such a framework, the constraints in (1d) are as follows. For feeder 1: $x_1^1 + x_1^2 + x_1^3 \leq c_1^1$, $x_2^2 + x_2^3 \leq c_2^1$, and $x_3^3 \leq c_3^1$; for feeder 2: $x_1^1 \leq c_1^2$; for feeder 3: $x_1^2 + x_1^3 \leq c_1^3$, $x_2^2 + x_2^3 \leq c_2^3$, and $x_3^3 \leq c_3^3$; for feeder 4: $x_1^2 \leq c_1^4$, and $x_2^2 \leq c_2^4$; and, finally, for feeder 5: $x_1^3 \leq c_1^5$, $x_2^3 \leq c_2^5$, and $x_3^3 \leq c_3^5$. □

Example 2 (Optimization objectives): Perhaps the simplest optimization problem that might be considered under the proposed framework is

$$\min_{\mathbf{x} \in \mathcal{X}} \quad J_{chg}(\mathbf{x}) := \frac{1}{2} \sum_{i \in \mathcal{V}} \left(x_0^i\right)^2. \tag{3}$$

Solving such a problem means that the PEVs will charge as much as possible while satisfying the constraints in (1). Clearly, $J_{chg}(\cdot)$ satisfies Standing Assumptions 1 and 2 (note that $\partial J_{chg}(\mathbf{x})/\partial x_0^i = x_0^i$ relies only on local information of the i-th PEV). Moreover, although $J_{chg}(\cdot)$ is separable over the PEVs, the optimization problem in (3) is still coupled over the fleet of PEVs due to the constraints in (1d).

Another optimization problem that could be considered is

$$\min_{\mathbf{x} \in \mathcal{X}} \quad J(\mathbf{x}) := J_{chg}(\mathbf{x}) + J_{ref}(\mathbf{x}) + J_{deg}(\mathbf{x}), \tag{4}$$

where $J_{chg}(\cdot)$ is defined as in (3), and

$$J_{ref}(\mathbf{x}) = \frac{1}{2}\sum_{k\in\mathcal{T}}\left(r_k - \sum_{i\in\mathcal{V}_k} x_k^i\right)^2,$$
$$J_{deg}(\mathbf{x}) = \frac{1}{2}\sum_{i\in\mathcal{V}}\sum_{k\in\mathcal{T}^i}\left(\alpha^i\left(x_k^i\right)^2 + \beta^i x_k^i + \gamma^i\right).$$

Here, $J_{ref}(\cdot)$ is a cost associated to the deviation from a reference demand profile[1], and $r_k \in \mathbb{R}_{\geq 0}$ is the reference demand (in kW) to be consumed by the fleet of PEVs over the time interval $k \in \mathcal{T}$ (it is assumed that r_k, for all $k \in \mathcal{T}$, is broadcast by the aggregator to the PEVs). In contrast, $J_{deg}(\cdot)$ is a cost associated to the battery degradation[2] of the PEVs, and $\alpha^i, \beta^i, \gamma^i \in \mathbb{R}_{>0}$ are constants that depend on the voltage and energy capacity parameters of the battery of the i-th PEV.

Clearly, the cost function $J(\cdot)$ defined in (4) is convex and twice continuously differentiable. Hence, Standing Assumption 1 holds under such a cost. Moreover, note that

$$\frac{\partial J(\mathbf{x})}{\partial x_0^j} = x_0^j, \quad \forall j \in \mathcal{V},$$
$$\frac{\partial J(\mathbf{x})}{\partial x_l^j} = -r_l + \sum_{i\in\mathcal{V}_l} x_l^i + \alpha^j x_l^j + \frac{\beta^j}{2}, \quad \forall l \in \mathcal{T}^j, \quad \forall j \in \mathcal{V}.$$

Here, notice that besides the reference profile r_l and the aggregated term $\sum_{i\in\mathcal{V}_l} x_l^i$, all of the other terms in $\partial J(\mathbf{x})/\partial x_l^j$ depend only on individual information of the j-th PEV. Furthermore, since the aggregator is able to send distribution network-level variables and aggregated power profiles, the information regarding r_l and $\sum_{i\in\mathcal{V}_l} x_l^i$, for all $l \in \mathcal{T}$, is also available at every PEV. Therefore, Standing Assumption 2 also holds under the cost defined in (4).

Finally, notice that in (4) one could replace $J_{ref}(\mathbf{x})$ with $J_{dem}(\mathbf{x}) = (1/2)\sum_{k\in\mathcal{T}}\left(D_k + \sum_{i\in\mathcal{V}_k} x_k^i\right)^2$, where D_k denotes the aggregated non-PEV demand at the time slot $k \in \mathcal{T}$ (broadcast by the aggregator to the PEVs), and thus consider the same optimization objectives as in [9], [10], [11], [12], [15], [16]. □

III. Real-Time Decentralized Charging Control

In this section, we design a continuous-time optimization-based control law to coordinate the charging process of a fleet of PEVs in real time. The main motivation behind such a real-time approach is its capability to respond, in the sense of disturbance rejection, to unexpected arrivals or departures of the PEVs [8]. Throughout, let

$$g_{d,k}^i(x_k^i) = x_k^i - d^i, \quad \forall k \in \mathcal{T}^i, \quad \forall i \in \mathcal{V},$$
$$g_{c,k}^z(\mathbf{x}) = \sum_{j\in\mathcal{V}_k} \psi^{z,j} x_k^j - c_k^z, \quad \forall k \in \mathcal{T}, \quad \forall z \in \mathcal{F}.$$

[1]Such a reference demand profile might be related, for instance, to some power bought by the electricity provider in a day-ahead market or to some forecast energy profile [26], [27].

[2]The considered cost $J_{deg}(\cdot)$ is consistent with battery degradation cost models of LiFePO4 battery cells [28], e.g., [9, Equation (7)], [10, Equation (5)], [12, Equation (9)].

Using these functions, the constraints in (1b) can be written as $g_{d,k}^i(x_k^i) \leq 0$, and the constraints in (1d) as $g_{c,k}^z(\mathbf{x}) \leq 0$. Here, the sub-indices $_d$ and $_c$ are to differentiate decoupled and coupled constraints, respectively. Finally, following such a notation, let $y_{d,k}^i \in \mathbb{R}_{\geq 0}$ and $y_{c,k}^z \in \mathbb{R}_{\geq 0}$ denote the Lagrange multipliers associated to the constraints $g_{d,k}^i(x_k^i) \leq 0$ and $g_{c,k}^z(\mathbf{x}) \leq 0$, respectively.

Our proposed approach is as follows. Let $t \in \mathbb{R}_{\geq 0}$ denote the continuous-time variable representing the current (continuous) time, and let the charging dynamics of the PEVs be characterized by

$$\dot{e}^i(t) = -\eta^i u^i(t) \quad \text{[with initial condition } e^i(0) \in \mathbb{R}_{\geq 0}\text{]},$$

for all $i \in \mathcal{V}$, where $u^i(t) \in \mathbb{R}_{\geq 0}$ denote the charging power (in kW) that is currently applied to the PEV $i \in \mathcal{V}$. We set

$$w^z(t) = \frac{c_1^z}{\max\left\{c_1^z,\, \sum_{j\in\mathcal{V}_1} \psi^{z,j} x_1^j(t)\right\}}, \quad \forall z \in \mathcal{F}, \tag{5a}$$
$$v^i(t) = \min_{\zeta\in\{z\in\mathcal{F}\,:\,\psi^{z,i}=1\}} w^\zeta(t), \quad \forall i \in \mathcal{V}, \tag{5b}$$
$$u^i(t) = \min\left\{v^i(t) x_1^i(t),\, d^i\right\}, \quad \forall i \in \mathcal{V}, \tag{5c}$$

where $x_1^i(t)$ is the value of the optimization variable x_1^i at time t; $w^z(t)$ quantifies the capacity violation of the z-th feeder at the time slot 1 under the collective scheduled charging profile $\mathbf{x}(t)$ (in particular, note that $0 < w^z(t) \leq 1$, for all $z \in \mathcal{F}$); and $v^i(t)$ is a scaling factor to scale down the value $x_1^i(t)$ for the i-th PEV according to the relevant feeder capacity violations. Under such a mapping, it follows that $u^i(t) \geq 0$ whenever $x_1^i(t) \geq 0$, for all $i \in \mathcal{V}$; $\sum_{i\in\mathcal{V}_1} \psi^{z,i} u^i(t) \leq c_1^z$, for all $z \in \mathcal{F}$; $u^i(t) \leq d^i$, for all $i \in \mathcal{V}$; and $u^i(t) \leq x_1^i(t)$ with $u^i(t) = x_1^i(t)$ whenever $\mathbf{x}(t) \in \mathcal{X}$, for all $i \in \mathcal{V}$. Hence, under the control law in (5), the power capacity constraints of the system are satisfied for the present time slot $k = 1$ (c.f., (1b) and (1d)), and, whenever $\mathbf{x}(t)$ is feasible it holds that $u^i(t) = x_1^i(t)$, for all $i \in \mathcal{V}$. Moreover, note that $w^z(t)$ in (5a) is a distribution network-level variable, and thus can be sent to the PEVs by the aggregator (c.f., Standing Assumption 3). Consequently, the scaling factor $v^i(t)$ in (5b) and the control law $u^i(t)$ in (5c) can be computed locally at the i-th PEV.

Considering the aforementioned control law, we thus need to design some continuous-time optimization dynamics to update $x_k^i(t)$, for all $k \in \mathcal{T}_e^i$ and all $i \in \mathcal{V}$, that

(C1) satisfy the decentralized structure of the system;

(C2) satisfy the constraints in (1a) and (1c) for all $t \geq 0$;

(C3) converge to the solution of (2).

Notice that Condition C2 is important to exclude negative $u^i(t)$ values and to avoid overcharging the batteries of the PEVs. In what follows, we proceed to design some continuous-time optimization dynamics that satisfy all three conditions.

A. Continuous-Time Optimization Dynamics

In this section we proceed to design a continuous-time dynamical system to update the optimization variables $x_k^i(t)$, for all $k \in \mathcal{T}_e^i$, all $i \in \mathcal{V}$, and all $t \geq 0$. To formulate such a dynamical system, we rely on the ideas of population games [18] and payoff dynamics models [20].

The field of population games regards a continuum of players that interact with each other in a strategic scenario. The seminal work of [18] has shown that, under certain mild assumptions, the temporal evolution of the (mean) strategic distribution of the population of players can be approximated through some ordinary differential equations (ODEs). Hence, the decision-making dynamics of the population of players can be studied by analyzing the corresponding nonlinear ODEs. Our interest on such population dynamics is that the resulting ODEs have certain invariance properties that can used to directly handle some of the constraints in (1). More precisely, the constraints in (1a) and (1c). On the other hand, the recent work of [20] has extended the aforementioned ideas of population games to include payoff dynamics models, where the payoff signals of the game are governed by a continuous-time dynamical system. By doing so, the framework of payoff dynamics models allows the consideration of more elaborate strategic interaction scenarios. In our recent publication [21], we have exploited such ideas for generalized Nash equilibrium seeking in population games under equality constraints. Following a similar approach, in this paper we exploit the ideas of payoff dynamics models to design a continuous-time dynamical system to solve (2) satisfying the constraints in (1a) and (1c) along the trajectories of the system, i.e., for all $t \geq 0$ (recall Condition C2). In contrast with [21], however, the model proposed in this paper allows the consideration of inequality constraints (in this case, (1b) and (1d)).

Based on these ideas, we design a novel form of continuous-time primal-dual optimization dynamics that satisfy Conditions C1, C2, and C3. The proposed dynamics are as follows. On one hand, every PEV $i \in \mathcal{V}$ updates its variables x_k^i, for all $k \in \mathcal{T}_e^i$, as well as the variables $y_{d,k}^i$, for all $k \in \mathcal{T}^i$, according to the dynamics

$$\dot{x}_k^i(t) = \sum_{l \in \mathcal{T}_e^i} x_l^i(t)\rho_{lk}^i(t) - x_k^i(t) \sum_{l \in \mathcal{T}_e^i} \rho_{kl}^i(t), \tag{6a}$$

$$\dot{y}_{d,k}^i(t) = \left[g_{d,k}^i\left(x_k^i(t)\right)\right]_+ - y_{d,k}^i(t)\left[-g_{d,k}^i\left(x_k^i(t)\right)\right]_+, \tag{6b}$$

with $[\cdot]_+ \triangleq \max\{\cdot, 0\}$, and

$$\rho_{kl}^i(t) = \left[p_l^i(t) - p_k^i(t)\right]_+, \quad \forall k,l \in \mathcal{T}_e^i,$$

$$p_k^i(t) = -\frac{\partial J(\mathbf{x}(t))}{\partial x_k^i} - y_{d,k}^i(t) - \sum_{z \in \mathcal{F}} y_{c,k}^z(t)\psi^{z,i}, \quad \forall k \in \mathcal{T}^i,$$

$$p_0^i(t) = -\frac{\partial J\left(\mathbf{x}(t)\right)}{\partial x_0^i}.$$

On the other hand, the aggregator updates the variables $y_{c,k}^z$, for all $k \in \mathcal{T}$ and all $z \in \mathcal{F}$, according to the dynamics

$$\dot{y}_{c,k}^z(t) = \left[g_{c,k}^z\left(\mathbf{x}(t)\right)\right]_+ - y_{c,k}^z(t)\left[-g_{c,k}^z\left(\mathbf{x}(t)\right)\right]_+. \tag{7}$$

Notice that the variables $y_{c,k}^z$, for all $k \in \mathcal{T}$ and all $z \in \mathcal{F}$, are distribution network-level variables, and, therefore, can be broadcast by the aggregator to the fleet of PEVs. Hence, under Standing Assumptions 2 and 3, the proposed dynamics can indeed be computed in the considered decentralized fashion, and thus satisfy Condition C1. Moreover, note that the number of optimization variables that the aggregator must update, i.e., $y_{c,k}^z$, for all $k \in \mathcal{T}$ and all $z \in \mathcal{F}$, is independent of the number of PEVs. Hence, the local computational complexity (in terms of local computation resources) is independent of the number of PEVs. Consequently, the proposed framework is scalable to large PEV fleets. Furthermore, to exploit the invariance properties the proposed dynamics, we impose the following conditions on the initial state of the dynamical system.

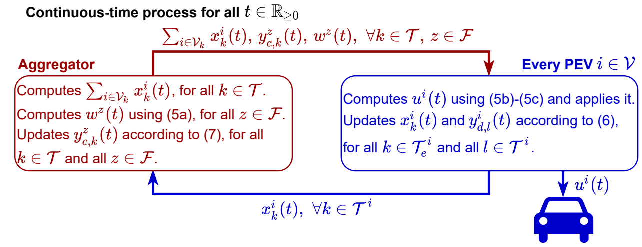

Fig. 2. Considered real-time optimization and control scheme. Notice that, depending on the objective $J(\mathbf{x})$, the aggregator may also send other distribution network-level variables to the PEVs (c.f., Example 2).

Standing Assumption 4: Let i) $x_k^i(0) \geq 0$, for all $k \in \mathcal{T}_e^i$ and all $i \in \mathcal{V}$; ii) $\sum_{k\in\mathcal{T}_e^i} x_k^i(0) = e^i(0)/(\eta^i\delta)$, for all $i \in \mathcal{V}$; iii) $y_{d,k}^i(0) \geq 0$, for all $k \in \mathcal{T}^i$ and all $i \in \mathcal{V}$; and iv) $y_{c,k}^z(0) \geq 0$, for all $k \in \mathcal{T}$ and all $z \in \mathcal{F}$. □

For the sake of clarity, the considered continuous-time optimization and control scheme is summarized in Fig. 2. We now proceed to analyze the proposed continuous-time optimization dynamics.

IV. Analysis of the Proposed Continuous-Time Optimization Dynamics

In this section, we characterize the invariance properties and the equilibria set of the dynamics in (6)-(7), and we show that such dynamics solve the optimization problem in (2). That is, the set of solutions of (2) is asymptotically stable under (6)-(7). Throughout, let

$$\mathbf{y}_d^i = \left[y_{d,1}^i,\, y_{d,2}^i, \cdots, y_{d,n_{\mathcal{T}^i}}^i\right]^\top \in \mathbb{R}^{n_{\mathcal{T}^i}},$$

$$\mathbf{y}_c^z = \left[y_{c,1}^z,\, y_{c,2}^z, \cdots, y_{c,n_{\mathcal{T}}}^z\right]^\top \in \mathbb{R}^{n_{\mathcal{T}}},$$

$$\mathbf{y} = \left[\mathbf{y}_d^1,\, \mathbf{y}_d^2, \cdots, \mathbf{y}_d^{n_\mathcal{V}},\, \mathbf{y}_c^1,\, \mathbf{y}_c^2, \cdots, \mathbf{y}_c^{n_\mathcal{F}}\right]^\top \in \mathbb{R}^{n_\mathcal{Q}},$$

where $n_\mathcal{T} = \max_{i\in\mathcal{V}} n_{\mathcal{T}^i}$ and $n_\mathcal{Q} = \sum_{i\in\mathcal{V}} n_{\mathcal{T}^i} + n_\mathcal{F} n_\mathcal{T}$, and let $\Delta = \left\{\mathbf{x} \in \mathbb{R}_{\geq 0}^n : \sum_{k\in\mathcal{T}_e^i} x_k^i = e^i(0)/(\eta^i\delta),\ \forall i \in \mathcal{V}\right\}$. Namely, Δ is the set of vectors $\mathbf{x}$ that satisfies the constraints in (1a) and (1c).

A. Invariance Properties

In this subsection, we characterize some invariance properties of the proposed dynamics that allow the satisfaction of the constraints in (1a) and (1c), as well as the ones regarding the non-negativity of the Lagrange multipliers, for all $t \geq 0$.

Proposition 1: Consider the dynamics in (6a). If $\mathbf{x}(0) \in \Delta$, then $\mathbf{x}(t) \in \Delta$, for all $t \geq 0$. That is, Δ is positively invariant under the considered dynamics. $\square$

Proposition 2: Consider the dynamics in (6b) and (7). If $\mathbf{y}(0) \in \mathbb{R}^{n_{\mathcal{Q}}}_{\geq 0}$, then $\mathbf{y}(t) \in \mathbb{R}^{n_{\mathcal{Q}}}_{\geq 0}$ for all $t \geq 0$. That is, $\mathbb{R}^{n_{\mathcal{Q}}}_{\geq 0}$ is positively invariant under the considered dynamics. $\square$

Propositions 1 and 2, in conjunction with Standing Assumption 4, allow us to assert, without any additional loss of generality, that $\mathbf{x}(t) \in \Delta$ and $\mathbf{y}(t) \in \mathbb{R}^{n_{\mathcal{Q}}}_{\geq 0}$, for all $t \geq 0$. Hence, the proposed dynamics indeed satisfy Condition C2. Throughout, the reader should keep in mind that from now on we implicitly assume that $\mathbf{x}(\cdot) \in \Delta$ and $\mathbf{y}(\cdot) \in \mathbb{R}^{n_{\mathcal{Q}}}_{\geq 0}$.

B. Equilibria Set of the Proposed Dynamics

In this subsection, we show that the equilibria set of the dynamics (6)-(7) coincides with the set of solutions of the optimization problem in (2) and is asymptotically stable under the proposed dynamics. To provide such results, we introduce the following lemmas.

Lemma 1: Consider the dynamics in (6a) and let $\dot{\mathbf{x}}^i(t) = \left[\dot{x}^i_0(t), \dot{x}^i_1(t), \dot{x}^i_2(t), \cdots, \dot{x}^i_{n_{\mathcal{T}^i}}(t)\right] \in \mathbb{R}^{(n_{\mathcal{T}^i}+1)}$. Then, $\dot{\mathbf{x}}^i(t) = \mathbf{0}$, if and only if it holds that

$$x^i_k(t) > 0 \Rightarrow p^i_k(t) = \max_{l \in \mathcal{T}^i_e} p^i_l(t), \quad \forall k \in \mathcal{T}^i_e. \tag{8}$$

Here, $\mathbf{0}$ denotes the zero vector of appropriate dimension. $\square$

Lemma 2: Consider the dynamics in (6b) and let $\dot{\mathbf{y}}^i_d(t) = \left[\dot{y}^i_{d,1}(t), \dot{y}^i_{d,2}(t), \cdots, \dot{y}^i_{d,n_{\mathcal{T}^i}}(t)\right]^\top \in \mathbb{R}^{n_{\mathcal{T}^i}}$. Then, $\dot{\mathbf{y}}^i_d(t) = \mathbf{0}$, if and only if it holds that

$$x^i_k(t) \leq d^i \text{ and } y^i_{d,k}(t)\left(x^i_k(t) - d^i\right) = 0, \quad \forall k \in \mathcal{T}^i. \tag{9}$$

$\square$

Lemma 3: Consider the dynamics in (7) and let $\dot{\mathbf{y}}^z_c(t) = \left[\dot{y}^i_{c,1}(t), \dot{y}^i_{c,2}(t), \cdots, \dot{y}^z_{c,n_{\mathcal{T}}}(t)\right]^\top \in \mathbb{R}^{n_{\mathcal{T}}}$. Then, $\dot{\mathbf{y}}^z_c(t) = \mathbf{0}$, if and only if it holds that

$$\sum_{i \in \mathcal{V}_k} \psi^{z,i} x^i_k(t) \leq c^z_k \text{ and } y^z_{c,k}(t)\left(\sum_{i \in \mathcal{V}_k} \psi^{z,i} x^i_k(t) - c^z_k\right) = 0, \tag{10}$$

for all $k \in \mathcal{T}$. $\square$

Using Lemmas 1, 2, and 3, we now proceed to formally characterize the equilibria set of the dynamics in (6)-(7).

Theorem 1: Consider the dynamics in (6)-(7), and let

$$\mathcal{E} = \left\{ (\mathbf{x}, \mathbf{y}) \in \Delta \times \mathbb{R}^{n_{\mathcal{Q}}}_{\geq 0} \, : \begin{array}{l} \text{(8)-(9) hold for all } i \in \mathcal{V}, \\ \text{(10) holds for all } z \in \mathcal{F}. \end{array} \right\}. \tag{11}$$

Then, $(\mathbf{x}^*, \mathbf{y}^*) \in \Delta \times \mathbb{R}^{n_{\mathcal{Q}}}_{\geq 0}$ is an equilibrium point of the dynamics in (6)-(7) if and only if $(\mathbf{x}^*, \mathbf{y}^*) \in \mathcal{E}$. $\square$

Having characterized the equilibria set of the dynamics in (6)-(7), we now state the main results of this subsection.

Theorem 2: Consider the set $\mathcal{E}$ in (11) and the optimization problem in (2). The set $\mathcal{E}$ is nonempty, compact, and every point $(\mathbf{x}^*, \mathbf{y}^*) \in \mathcal{E}$ implies that $\mathbf{x}^* \in \arg\min_{\mathbf{x} \in \mathcal{X}} J(\mathbf{x})$. $\square$

Theorem 3: Consider the dynamics in (6)-(7) and the equilibria set $\mathcal{E}$ in (11). The set $\mathcal{E}$ is asymptotically stable under the considered dynamics. $\square$

Observe that Theorems 2 and 3 guarantee that the equilibria set of the dynamics in (6)-(7) is not only asymptotically stable, but also coincides with the set of solutions of the optimization problem in (2). In consequence, the proposed continuous-time optimization dynamics indeed satisfy Condition C3.

Remark 2: Note that in contrast with other related works, e.g., [12], the optimality and asymptotic stability results provided by Theorems 2 and 3 hold for arbitrary sizes of PEV fleets, and not only for the limiting case where the number of PEVs is assumed to be infinite (quite large). Hence, our proposed framework allows the consideration of a broader scope of applications.

V. Numerical Simulations

In this section, we apply our proposed method to a charging coordination scenario considering the distribution network of Fig. 1 and the optimization problem in (4). As illustration, we compare the dynamics in (6)-(7) against the continuous-time primal-dual gradient dynamics of [17] (with unitary time constants). Note that the continuous-time primal-dual gradient dynamics in [17] not only have exponential stability guarantees, but have been also considered in related network optimization and power-grid applications, e.g., [22], [23], [24]. Moreover, the dynamics in (6)-(7) can be computed using the same elementary linear algebra operations as the dynamics in [17]. For these reasons, we regard such dynamics as a relevant benchmark to compare our approach.

Consider a fleet with $n_{\mathcal{V}} = 40$ PEVs distributed as follows: 13 PEVs are connected at node B; 13 PEVs are connected at node D; and 14 PEVs are connected at node E. We consider the charging coordination over the time period from 19:00 to 7:00, we let $\delta = 1$, and we sample the charging horizons according to the (truncated) normal distribution $n_{\mathcal{T}^i} \sim \mathcal{N}(5{:}00, 4\delta^2)$, for all $i \in \mathcal{V}$. Namely, for our simulations we have $n_{\mathcal{T}} = 12$. Besides, the PEVs are assumed to be heterogeneous, and, without loss of generality, the corresponding parameters are uniformly sampled for all $i \in \mathcal{V}$ as follows: $d^i \sim \mathcal{U}(2, 4)$; $e^i(0) \sim \mathcal{U}(5, 20)$; $\eta^i \sim \mathcal{U}(0.8, 0.9)$; $\alpha^i \sim \mathcal{U}(0.003, 0.005)$; $\beta^i \sim \mathcal{U}(0.06, 0.09)$; and $\gamma^i \sim \mathcal{U}(0.002, 0.004)$. In particular, notice that the battery degradation cost parameters are consistent with the values reported in the literature [9]. Furthermore, regarding the capacities of the feeder lines, we set $c^1_k = 12$, $c^2_k = c^4_k = c^5_k = 3.6$, and $c^3_k = 6$, for all $k \in \{1, 2, 3\}$; and we set $c^1_k = 40$, $c^2_k = c^4_k = c^5_k = 12$, and $c^3_k = 20$, for all $k \in \{4, 5, \cdots, 12\}$. Finally, for the reference demand profile, we consider the one depicted in Fig. 3.

In Fig. 3, we provide the optimal collective scheduled charging profile for the aforementioned scenario, whilst in Figs. 4 and 5, we present the first 100s of the continuous-time behavior of the dynamics in (6)-(7) and [17] when applied to the considered scenario. Clearly, both continuous-time primal-dual gradient dynamics converge to the solution of the considered optimization problem with comparable performance. However, notice that while our proposed dynamics

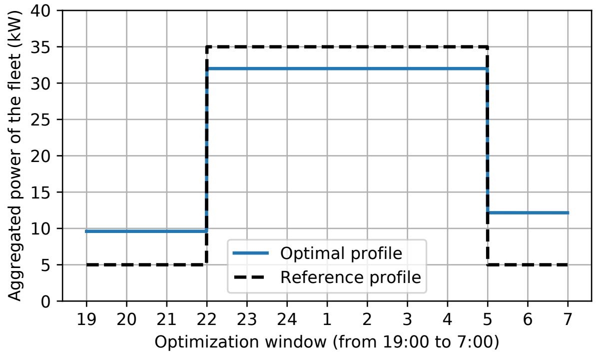

Fig. 3. Reference demand profile and optimal aggregated power profile of the fleet for the considered charging coordination problem.

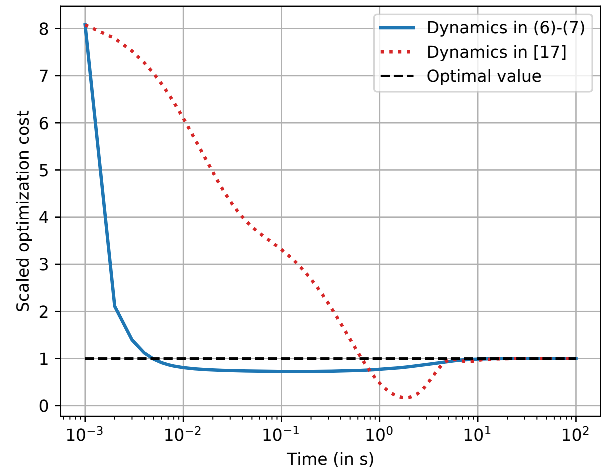

Fig. 4. Optimization cost $J(\mathbf{x}(t))$ over the first 100s of the continuous-time optimization process. All values are scaled over the optimal value.

(6)-(7) satisfy the constraints in (1a) and (1c) for all times, the dynamics in [17] do not satisfy such constraints over the trajectories of the optimization process. This property of our dynamics has the following advantage. Notice that since the constraints in (1a) and (1c) are handled by the invariance properties of the dynamics in (6a), to solve the considered optimization problem using (6)-(7) it is not necessary to compute or update any dual Lagrange multipliers associated to such constraints. Hence, the total number of optimization variables that are considered with the dynamics in (6)-(7) is given by $n+n_{\mathcal{Q}}$. In contrast, the total number of optimization variables that are considered with the dynamics of [17] is $2n+n_{\mathcal{Q}}+n_{\mathcal{V}}$ (which requires for each PEV to compute and update $n_{\mathcal{T}^i}+2$ additional optimization variables). Therefore, when compared to the dynamics of [17], our proposed dynamics reduce the computational load on the i-th PEV by computing $n_{\mathcal{T}^i}+2$ less variables. This is of especial importance in charging coordination scenarios with small δ and large $n_{\mathcal{T}}$ values, i.e., under shorter time slots and larger horizons.

Now, to illustrate the performance of the proposed real-time control method under uncertain departures of the PEVs, consider the aforementioned scenario, but assume that 10 randomly selected vehicles depart from their charging stations at time $t = 100$s. As shown in Figs. 6 and 7, the proposed real-time control strategy allows for the remaining PEVs to readjust their charging profiles in real time without violating the capacity constraints of the feeder lines. Hence, the fleet of PEVs effectively responds in real time to the corresponding disturbance.

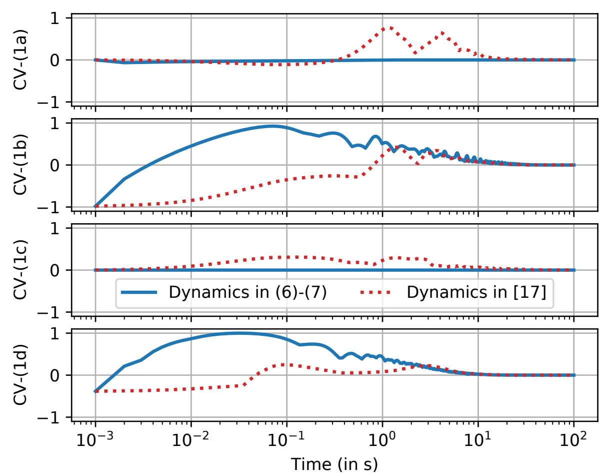

Fig. 5. Constraints violations over the first 100s of the continuous-time optimization process. CV-(1a) is computed as $\max_{k\in\mathcal{T}_e^i,\, i\in\mathcal{V}} -x_k^i(t)$; CV-(1b) is computed as $\max_{k\in\mathcal{T}^i,\, i\in\mathcal{V}} g_{d,k}^i\left(x_k^i(t)\right)$; CV-(1c) is computed as $\max_{i\in\mathcal{V}} \left|\mathbf{1}^\top \mathbf{x}^i(t) - e^i(0)/\eta^i\delta\right|$, where $\mathbf{1}$ is the vector of ones with appropriate dimension; and, finally, CV-(1d) is computed as $\max_{k\in\mathcal{T},\, z\in\mathcal{F}} g_{c,k}^z\left(\mathbf{x}(t)\right)$. Hence, positive values of the CV terms coincide with constraints violations. All values are scaled to $[-1, 1]$.

VI. Concluding Remarks and Future Work

This paper has proposed a novel method for the decentralized real-time charging coordination of PEVs, which is a crucial technology for future smart-city networks. Relying on recent ideas in the fields of population games and payoff dynamics models, we have developed a novel form of continuous-time primal-dual gradient dynamics, and we have

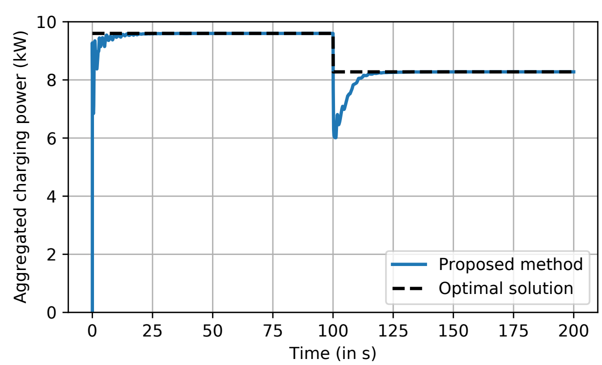

Fig. 6. Aggregated charging power given by $\sum_{i\in\mathcal{V}_1} u^i(t)$.

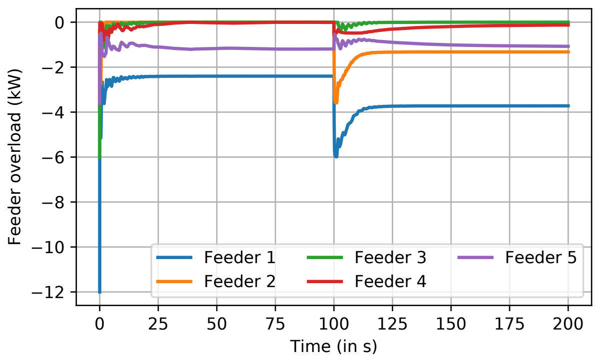

Fig. 7. The feeder overloads are given by $\sum_{i\in\mathcal{V}_1}\psi^{z,i}u^i(t)-c_1^z$, for all $z\in\mathcal{F}$. Hence, positive values coincide with feeder overloads.

proposed a real-time control method to compute the charging powers of the PEVs in a decentralized fashion and under (hard) feeder capacity constraints. The optimality and asymptotic stability of the proposed dynamics has been formally proven through nonlinear analyses, and the advantages of the proposed method have been illustrated through numerical simulations.

Future work should focus on the consideration of some practical implementation details as time delays in the communications with the aggregator, as well as on the characterization of the convergence rate of the proposed optimization dynamics.

Appendix

A. Proof of Proposition 1

Note that

$$\sum_{k\in\mathcal{T}_e^i}\dot{x}_k^i(t)=\sum_{k\in\mathcal{T}_e^i}\sum_{l\in\mathcal{T}_e^i}x_l^i(t)\rho_{lk}^i(t)-\sum_{k\in\mathcal{T}_e^i}\sum_{l\in\mathcal{T}_e^i}x_k^i(t)\rho_{kl}^i(t)$$
$$=0.$$

Hence, $\sum_{k\in\mathcal{T}_e^i}x_k^i(0)=m^i\Rightarrow\sum_{k\in\mathcal{T}_e^i}x_k^i(t)=m^i,\forall t\geq 0$, where $m^i=e^i(0)/(\eta^i\delta)$. Additionally, if $x_k^i(t)=0$, then $\dot{x}_k^i(t)\geq 0$. Thus, $x_k^i(0)\geq 0$ implies that $x_k^i(t)\geq 0$, for all $t\geq 0$. Since this holds for every $k\in\mathcal{T}_e^i$ and $i\in\mathcal{V}$, Δ is indeed positively invariant under the considered dynamics. ■

B. Proof of Proposition 2

Consider (6b) first. Notice that if $y_{d,k}^i(t)=0$, then $\dot{y}_{d,k}^i(t)\geq 0$. Hence, $y_{d,k}^i(0)\geq 0$ implies that $y_{d,k}^i(t)\geq 0$, for all $t\geq 0$. Considering (7), note that if $y_{c,k}^z(t)=0$, then $\dot{y}_{c,k}^z(t)\geq 0$. Thus, $y_{c,k}^z(0)\geq 0$ implies $y_{c,k}^z(t)\geq 0$, for all $t\geq 0$. Since these results hold for arbitrary k, i, and z, it holds that $\mathbf{y}(0)\in\mathbb{R}_{\geq 0}^{n_\mathcal{Q}}$ implies $\mathbf{y}(t)\in\mathbb{R}_{\geq 0}^{n_\mathcal{Q}}$, for all $t\geq 0$. ■

C. Proof of Lemma 1

(Sufficiency) Let (8) hold. Then, for all $a,b\in\mathcal{T}_e^i$ it holds that $x_a^i(t)\left[p_b^i(t)-p_a^i(t)\right]_+=0$. Thus, $\dot{\mathbf{x}}^i(t)=\mathbf{0}$.

(Necessity) Let $\dot{\mathbf{x}}^i(t)=\mathbf{0}$, but suppose that (8) does not hold. Also, let $a\in\mathcal{T}_e^i$ be such that $p_a^i(t)=\max_{l\in\mathcal{T}_e^i}p_l^i(t)$. Hence, $x_a^i(t)\left[p_b^i(t)-p_a^i(t)\right]_+=0$, for all $b\in\mathcal{T}_e^i$, and, therefore, $\dot{x}_a^i(t)=\sum_{b\in\mathcal{T}_e^i}x_b^i(t)\left[p_a^i(t)-p_b^i(t)\right]_+\geq 0$. Now, since (8) does not hold, there is some $b\in\mathcal{T}_e^i$ such that $x_b^i(t)>0$ and $p_b^i(t)<p_a^i(t)$. Consequently, $x_b^i(t)\left[p_a^i(t)-p_b^i(t)\right]_+>0$, $\dot{x}_a^i(t)>0$, and $\dot{\mathbf{x}}^i(t)\neq\mathbf{0}$, leading to a contradiction. ■

D. Proof of Lemma 2

(Sufficiency) Let (9) hold. Since $x_k^i(t)-d^i=g_{d,k}^i\left(x_k^i(t)\right)\leq 0$, it holds that $\dot{y}_{d,k}^i(t)=y_{d,k}^i(t)\left(x_k^i(t)-d^i\right)$, and, thus, $y_{d,k}^i(t)\left(x_k^i(t)-d^i\right)=0$ implies that $\dot{y}_{d,k}^i(t)=0$.

(Necessity) Let $\dot{\mathbf{y}}_d^i(t)=\mathbf{0}$, but suppose that (9) does not hold. Then, there is some $l\in\mathcal{T}^i$ such that either $x_l^i(t)>d^i$, or $y_{d,l}^i(t)\left(x_l^i(t)-d^i\right)\neq 0$. If $x_l^i(t)-d^i=g_{d,l}^i(x_l^i(t))>0$, then $\dot{y}_{d,l}^i(t)=x_l^i(t)-d^i>0$ and thus $\dot{\mathbf{y}}_d^i(t)\neq\mathbf{0}$. On the other hand, if $x_l^i(t)\leq d^i$ but $y_{d,l}^i(t)\left(x_l^i(t)-d^i\right)\neq 0$, then $\dot{y}_{d,l}^i(t)=y_{d,l}^i(t)\left(x_l^i(t)-d^i\right)\neq 0$ (in fact >0), and, again, $\dot{\mathbf{y}}_d^i(t)\neq\mathbf{0}$. This completes the proof by contradiction. ■

E. Proof of Lemma 3

The proof is analogous to the one of Lemma 2, but considers (7) instead of (6b), $y_{c,k}^z(t)$ instead of $y_{d,k}^i(t)$, and $g_{c,k}^z(\mathbf{x}(t))$ instead of $g_{d,k}^i(x_k^i(t))$. Hence, it is omitted. ■

F. Proof of Theorem 1

The result follows from Lemmas 1, 2, and 3. ■

G. Proof of Theorem 2

Let $\lambda_k^i\in\mathbb{R}_{\geq 0}$ denote the Lagrange multiplier associated to the constraint $x_k^i\geq 0$, for all $k\in\mathcal{T}_e^i$ and all $i\in\mathcal{V}$, and let $\nu^i\in\mathbb{R}$ be the Lagrange multiplier associated to the constraint $x_0^i+\sum_{k\in\mathcal{T}^i}x_k^i=e^i(0)/\left(\eta^i\delta\right)$, for all $i\in\mathcal{V}$. Also, let $\boldsymbol{\lambda}\in\mathbb{R}_{\geq 0}^{n}$ and $\boldsymbol{\nu}\in\mathbb{R}_{\geq 0}^{n_\mathcal{V}}$ be the vectors containing such Lagrange multipliers, respectively. Moreover, consider the set

$$\mathcal{K}=\left\{(\mathbf{x},\mathbf{y})\in\mathcal{X}\times\mathbb{R}_{\geq 0}^{n_\mathcal{Q}}:\begin{array}{c}(\mathbf{x},\mathbf{y},\boldsymbol{\lambda},\boldsymbol{\nu})\text{ satisfies (12) for}\\ \text{some }\boldsymbol{\lambda}\in\mathbb{R}_{\geq 0}^{n},\ \boldsymbol{\nu}\in\mathbb{R}^{n_\mathcal{V}}.\end{array}\right\},$$

where

$$\lambda_k^i x_k^i=0,\quad\forall k\in\mathcal{T}_e^i,\quad\forall i\in\mathcal{V},\tag{12a}$$
$$y_{d,k}^i g_{d,k}^i\left(x_k^i\right)=0,\quad\forall k\in\mathcal{T}^i,\quad\forall i\in\mathcal{V},\tag{12b}$$
$$y_{c,k}^z g_{c,k}^z\left(\mathbf{x}\right)=0,\quad\forall k\in\mathcal{T},\quad\forall z\in\mathcal{F},\tag{12c}$$
$$-\frac{\partial J(\mathbf{x})}{\partial x_k^i}-\phi_k^i=\nu^i-\lambda_k^i,\quad\forall k\in\mathcal{T}_e^i,\quad\forall i\in\mathcal{V},\tag{12d}$$

with $\phi_0^i=0$, and $\phi_k^i=y_{d,k}^i+\sum_{z\in\mathcal{F}}y_{c,k}^z\psi^{z,i}$ if $k\in\mathcal{T}^i$, for all $i\in\mathcal{V}$. Namely, $\mathcal{K}$ is the set of vectors $\mathbf{x}$ and $\mathbf{y}$ that satisfy the KKT optimality conditions for the optimization problem in (2). We now prove that $(\mathbf{x}^*,\mathbf{y}^*)\in\mathcal{E}$ if and only if $(\mathbf{x}^*,\mathbf{y}^*)\in\mathcal{K}$.

(Sufficiency) Let $(\mathbf{x}^*,\mathbf{y}^*)\in\mathcal{K}$. Note that $(\mathbf{x}^*,\mathbf{y}^*)\in\mathcal{X}\times\mathbb{R}_{\geq 0}^{n_\mathcal{Q}}$ implies that $\mathbf{x}^*\in\Delta$ and $\mathbf{y}^*\in\mathbb{R}_{\geq 0}^{n_\mathcal{Q}}$. Then, (12b) implies that (9) holds for all $i\in\mathcal{V}$, and (12c) implies that (10) holds for all $z\in\mathcal{F}$. Also, $p_k^{i*}=-\partial J(\mathbf{x}^*)/\partial x_k^{i*}-\phi_k^{i*}$, for all $k\in\mathcal{T}_e^i$ and all $i\in\mathcal{V}$. Consequently, (12a) and

(12d) imply that $p_k^{i*} = \nu^{i*}$, for all $k \in \operatorname{supp}(\mathbf{x}^*)$ and all $i \in \mathcal{V}$. Similarly, since $\boldsymbol{\lambda}^* \in \mathbb{R}^n_{\geq 0}$, condition (12d) implies that $p_l^{i*} = \nu^{i*} - \lambda_l^{i*} \leq \nu^{i*}$, for all $l \in \mathcal{T}_e^i$ and all $i \in \mathcal{V}$. Therefore, for all $k \in \operatorname{supp}(\mathbf{x}^*)$ and all $i \in \mathcal{V}$, it holds that $p_k^{i*} = \max_{l \in \mathcal{T}_e^i} p_l^{i*}$, and so (8) holds for all $i \in \mathcal{V}$. Hence, $(\mathbf{x}^*, \mathbf{y}^*) \in \mathcal{E}$.

(Necessity) Let $(\mathbf{x}^*, \mathbf{y}^*) \in \mathcal{E}$. Clearly, $(\mathbf{x}^*, \mathbf{y}^*) \in \mathcal{E}$ implies that $\mathbf{x}^* \in \mathcal{X}$, that $\mathbf{y}^* \in \mathbb{R}^{n_\mathcal{Q}}_{\geq 0}$, and that (12b) and (12c) hold. Now, pick $\nu^{i*} = \max_{l \in \mathcal{T}_e^i} p_l^{i*}$ and $\lambda_k^{i*} = \nu^{i*} - p_k^{i*}$, for all $k \in \mathcal{T}_e^i$ and all $i \in \mathcal{V}$. Under such a selection, and due to the fact that (8) holds, it follows that (12a) and (12d) hold and that $\boldsymbol{\lambda}^* \in \mathbb{R}^n_{\geq 0}$. Consequently, $(\mathbf{x}^*, \mathbf{y}^*) \in \mathcal{K}$.

Therefore, since $\mathcal{E} = \mathcal{K}$ and $\mathcal{K}$ is the set of KKT points of the convex optimization problem in (2) (which has nonempty and compact feasible set $\mathcal{X}$, satisfies the Slater's condition, and has continuous objective function $J(\cdot)$), it follows that $\mathcal{E}$ is nonempty, compact[3], and every point $(\mathbf{x}^*, \mathbf{y}^*) \in \mathcal{E}$ satisfies that $\mathbf{x}^* \in \arg\min_{\mathbf{x} \in \mathcal{X}} J(\mathbf{x})$. ■

H. Proof of Theorem 3

To present the proof more compactly, let $\mathbf{x} \triangleq \mathbf{x}(t)$, $\mathbf{y} \triangleq \mathbf{y}(t)$, $p_k^i \triangleq p_k^i(t)$ for all $k \in \mathcal{T}_e^i$ and all $i \in \mathcal{V}$, $g_{d,k}^i \triangleq g_{d,k}^i\left(x_k^i\right)$ for all $k \in \mathcal{T}^i$ and all $i \in \mathcal{V}$, $g_{c,k}^z \triangleq g_{c,k}^z(\mathbf{x})$ for all $k \in \mathcal{T}$ and all $z \in \mathcal{F}$, and $J \triangleq J(\mathbf{x})$. Moreover, let

$$\begin{aligned}
\mathbf{g}_d^i &\triangleq \left[g_{d,1}^i,\, g_{d,2}^i, \cdots, g_{d,n_{\mathcal{T}^i}}^i\right]^\top \in \mathbb{R}^{n_{\mathcal{T}^i}}, \quad \forall i \in \mathcal{V} \\
\mathbf{g}_c^z &\triangleq \left[g_{c,1}^z,\, g_{c,2}^z, \cdots, g_{c,n_\mathcal{T}}^z\right]^\top \in \mathbb{R}^{n_\mathcal{T}}, \quad \forall z \in \mathcal{F} \\
\mathbf{g} &\triangleq \left[\mathbf{g}_d^1, \mathbf{g}_d^2, \cdots, \mathbf{g}_d^{n_\mathcal{V}}, \mathbf{g}_c^1, \mathbf{g}_c^2 \cdots, \mathbf{g}_c^{n_\mathcal{F}}\right]^\top \in \mathbb{R}^{n_\mathcal{Q}}.
\end{aligned}$$

Notice that the elements of $\mathbf{g}$ preserve the same ordering as the ones of $\mathbf{y}$. Thus, let $\mathcal{Q} = \{1, 2, \ldots, n_\mathcal{Q}\}$ be the set of indices pointing to the elements of $\mathbf{y}$ and $\mathbf{g}$, and, for all $q \in \mathcal{Q}$, let $y_{[q]} \in \mathbb{R}$ and $g_{[q]} \in \mathbb{R}$ denote the q-th element of $\mathbf{y}$ and $\mathbf{g}$, respectively. In consequence, from (6b) and (7), we have that

$$\dot{y}_{[q]} = \left[g_{[q]}\right]_+ - y_{[q]}\left[-g_{[q]}\right]_+, \quad \forall q \in \mathcal{Q}. \tag{13}$$

Also, under such a notation, it follows that

$$p_k^i = -\frac{\partial J}{\partial x_k^i} - \sum_{q \in \mathcal{Q}} y_{[q]} \frac{\partial g_{[q]}}{\partial x_k^i}, \quad \forall k \in \mathcal{T}_e^i, \quad \forall i \in \mathcal{V}. \tag{14}$$

Now, consider the function

$$V(\mathbf{x}, \mathbf{y}) = \underbrace{\sum_{i \in \mathcal{V}} \sum_{l \in \mathcal{T}_e^i} \sum_{k \in \mathcal{T}_e^i} x_k^i P_{kl}^i(\mathbf{x}, \mathbf{y})}_{V_x(\mathbf{x}, \mathbf{y})} + \underbrace{\sum_{q \in \mathcal{Q}} G_q(\mathbf{x}, \mathbf{y})}_{V_y(\mathbf{x}, \mathbf{y})},$$

where

$$\begin{aligned}
P_{kl}^i(\mathbf{x}, \mathbf{y}) &= \int_0^{p_l^i - p_k^i} [\sigma]_+ \, d\sigma, \quad \forall k, l \in \mathcal{T}_e^i, \quad \forall i \in \mathcal{V}, \\
G_q(\mathbf{x}, \mathbf{y}) &= \int_0^{g_{[q]}} [\sigma]_+ \, d\sigma + y_{[q]} \int_0^{-g_{[q]}} [\sigma]_+ \, d\sigma, \quad \forall q \in \mathcal{Q}.
\end{aligned}$$

[3]The compactness of $\mathcal{E}$ can be proven using analogous arguments as in [21, Proposition 3].

Clearly, $V_x(\mathbf{x}, \mathbf{y}) \geq 0$ and $V_y(\mathbf{x}, \mathbf{y}) \geq 0$ for all $(\mathbf{x}, \mathbf{y}) \in \Delta \times \mathbb{R}^{n_\mathcal{Q}}_{\geq 0}$. Moreover, following a similar analysis as in [18, Theorem 7.2.9], it is straightforward to check that $V_x(\mathbf{x}, \mathbf{y}) = 0$ if and only if (8) holds. Furthermore, observe that $V_y(\mathbf{x}, \mathbf{y}) = 0$ if and only if (9) and (10) hold. Consequently, $V(\mathbf{x}, \mathbf{y}) = 0$ if and only if $(\mathbf{x}, \mathbf{y}) \in \mathcal{E}$. Thus, $V(\cdot, \cdot)$ serves as a valid Lyapunov function candidate to investigate the stability properties of $\mathcal{E}$ (c.f., [29, Corollary 4.7]). Therefore, we proceed to analyze its derivatives. In particular, we have that

$$\begin{aligned}
\frac{\partial V}{\partial x_b^a} &= \sum_{l \in \mathcal{T}_e^a} \mathrm{P}_{bl}^a + \sum_{i \in \mathcal{V}} \sum_{l \in \mathcal{T}_e^i} \sum_{k \in \mathcal{T}_e^i} x_k^i \frac{\partial \mathrm{P}_{kl}^i}{\partial x_b^a} + \sum_{q \in \mathcal{Q}} \frac{\partial G_q}{\partial x_b^a} \\
\frac{\partial V}{\partial y_{[h]}} &= \sum_{i \in \mathcal{V}} \sum_{l \in \mathcal{T}_e^i} \sum_{k \in \mathcal{T}_e^i} x_k^i \frac{\partial \mathrm{P}_{kl}^i}{\partial y_{[h]}} + \int_0^{-g_{[h]}} [\sigma]_+ \, d\sigma,
\end{aligned}$$

for all $a \in \mathcal{V}$, all $b \in \mathcal{T}_e^a$, and all $h \in \mathcal{Q}$. Here, we have defined $V \triangleq V(\mathbf{x}, \mathbf{y})$, $P_{kl}^i \triangleq P_{kl}^i(\mathbf{x}, \mathbf{y})$, and $G_q \triangleq G_q(\mathbf{x}, \mathbf{y})$. Moreover,

$$\begin{aligned}
\sum_{i \in \mathcal{V}} \sum_{l, k \in \mathcal{T}_e^i} x_k^i \frac{\partial \mathrm{P}_{kl}^i}{\partial x_b^a} &= \sum_{i \in \mathcal{V}} \sum_{l, k \in \mathcal{T}_e^i} x_k^i \left[p_l^i - p_k^i\right]_+ \left(\frac{\partial p_l^i}{\partial x_b^a} - \frac{\partial p_k^i}{\partial x_b^a}\right) \\
&= \sum_{i \in \mathcal{V}} \sum_{l \in \mathcal{T}_e^i} \dot{x}_l^i \frac{\partial p_l^i}{\partial x_b^a} \quad \text{[using (6a)]}.
\end{aligned}$$

Similarly, observe that

$$\begin{aligned}
\sum_{q \in \mathcal{Q}} \frac{\partial G_q}{\partial x_b^a} &= \sum_{q \in \mathcal{Q}} \left(\left[g_{[q]}\right]_+ \frac{\partial g_{[q]}}{\partial x_b^a} - y_{[q]}\left[-g_{[q]}\right]_+ \frac{\partial g_{[q]}}{\partial x_b^a}\right) \\
&= \sum_{q \in \mathcal{Q}} \dot{y}_{[q]} \frac{\partial g_{[q]}}{\partial x_b^a}, \quad \text{[using (13)]}.
\end{aligned}$$

Finally, note that

$$\begin{aligned}
\sum_{k \in \mathcal{T}_e^i} x_k^i \frac{\partial \mathrm{P}_{kl}^i}{\partial y_{[h]}} &= \sum_{k \in \mathcal{T}_e^i} x_k^i \left[p_l^i - p_k^i\right]_+ \left(\frac{\partial p_l^i}{\partial y_{[h]}} - \frac{\partial p_k^i}{\partial y_{[h]}}\right) \\
&= \dot{x}_l^i \frac{\partial p_l^i}{\partial y_{[h]}} \quad \text{[using (6a)]} \\
&= -\dot{x}_l^i \frac{\partial g_{[h]}}{\partial x_l^i} \quad \text{[using (14)]},
\end{aligned}$$

and therefore,

$$\sum_{i \in \mathcal{V}} \sum_{l \in \mathcal{T}_e^i} \sum_{k \in \mathcal{T}_e^i} x_k^i \frac{\partial \mathrm{P}_{kl}^i}{\partial y_{[h]}} = -\sum_{i \in \mathcal{V}} \sum_{l \in \mathcal{T}_e^i} \dot{x}_l^i \frac{\partial g_{[h]}}{\partial x_l^i}.$$

Now, let

$$\boldsymbol{\Gamma}_P^j \triangleq \left[\sum_{l \in \mathcal{T}_e^j} P_{0l}^j, \sum_{l \in \mathcal{T}_e^j} P_{1l}^j, \cdots, \sum_{l \in \mathcal{T}_e^j} P_{n_{\mathcal{T}^j} l}^j\right]^\top \in \mathbb{R}^{(n_{\mathcal{T}^j}+1)}_{\geq 0},$$

for all $j \in \mathcal{V}$, and

$$\boldsymbol{\Gamma}_\mathrm{P} \triangleq \left[\left(\boldsymbol{\Gamma}_\mathrm{P}^1\right)^\top, \left(\boldsymbol{\Gamma}_\mathrm{P}^2\right)^\top, \cdots, \left(\boldsymbol{\Gamma}_\mathrm{P}^{n_\mathcal{V}}\right)^\top\right]^\top \in \mathbb{R}^n_{\geq 0}.$$

Similarly, let

$$\boldsymbol{\Gamma}_G \triangleq \left[\int_0^{-g_{[1]}} [\sigma]_+ d\sigma, \cdots, \int_0^{-g_{[n_\mathcal{Q}]}} [\sigma]_+ d\sigma\right]^\top \in \mathbb{R}^{n_\mathcal{Q}}_{\geq 0}.$$

Finally, let

$$\mathbf{p}^i \triangleq \left[p_0^i, p_1^i, \cdots, p_{n_{\mathcal{T}^i}}^i\right]^\top \in \mathbb{R}^{n_{\mathcal{T}^i}}, \quad \forall i \in \mathcal{V},$$
$$\mathbf{p} \triangleq \left[\mathbf{p}^1, \mathbf{p}^2, \cdots, \mathbf{p}^{n_\mathcal{V}}\right]^\top \in \mathbb{R}^n.$$

Under these formulations, it follows that

$$\nabla_{\mathbf{x}} V(\mathbf{x},\mathbf{y}) = \mathbf{\Gamma}_P + (\mathrm{D}\mathbf{p})^\top \dot{\mathbf{x}} + (\mathrm{D}\mathbf{g})^\top \dot{\mathbf{y}}$$
$$\nabla_{\mathbf{y}} V(\mathbf{x},\mathbf{y}) = \mathbf{\Gamma}_G - \mathrm{D}\mathbf{g}\dot{\mathbf{x}}.$$

Here, $\mathrm{D}\mathbf{p} \triangleq \mathrm{D}\mathbf{p}(\mathbf{x},\mathbf{y}) \in \mathbb{R}^{n\times n}$ is the Jacobian matrix $\mathbf{p}$ with respect to $\mathbf{x}$; and $\mathrm{D}\mathbf{g} \triangleq \mathrm{D}\mathbf{g}(\mathbf{x}) \in \mathbb{R}^{n_\mathcal{Q}\times n}$ is the Jacobian matrix of $\mathbf{g}$ with respect to $\mathbf{x}$. Therefore,

$$\begin{aligned}
&\left[\ (\nabla_{\mathbf{x}} V(\mathbf{x},\mathbf{y}))^\top, \quad (\nabla_{\mathbf{y}} V(\mathbf{x},\mathbf{y}))^\top\ \right]\left[\begin{array}{c}\dot{\mathbf{x}}\\ \dot{\mathbf{y}}\end{array}\right] \\
&\quad = \mathbf{\Gamma}_P^\top \dot{\mathbf{x}} + \dot{\mathbf{x}}^\top \mathrm{D}\mathbf{p}\dot{\mathbf{x}} + \dot{\mathbf{y}}^\top \mathrm{D}\mathbf{g}\dot{\mathbf{x}} + \mathbf{\Gamma}_G^\top \dot{\mathbf{y}} - \dot{\mathbf{x}}^\top (\mathrm{D}\mathbf{g})^\top \dot{\mathbf{y}} \\
&\quad = \mathbf{\Gamma}_P^\top \dot{\mathbf{x}} + \dot{\mathbf{x}}^\top \mathrm{D}\mathbf{p}\dot{\mathbf{x}} + \mathbf{\Gamma}_G^\top \dot{\mathbf{y}}.
\end{aligned}$$

Here, $\dot{\mathbf{x}}^\top (\mathrm{D}\mathbf{g})^\top \dot{\mathbf{y}} = \left(\dot{\mathbf{x}}^\top (\mathrm{D}\mathbf{g})^\top \dot{\mathbf{y}}\right)^\top = \dot{\mathbf{y}}^\top \mathrm{D}\mathbf{g}\dot{\mathbf{x}}$, since it is a scalar. Now, from the Standing Assumption 1 and the fact that $g_{[q]}$ is an affine function of $\mathbf{x}$, for all $q \in \mathcal{Q}$, it follows that $\mathrm{D}\mathbf{p}$ is a positive semi-definite matrix for all $\mathbf{x}$ and $\mathbf{y}$. Therefore, $\dot{\mathbf{x}}^\top \mathrm{D}\mathbf{p}\dot{\mathbf{x}} \le 0$ for all times. Moreover, since $\dot{\mathbf{x}} = \mathbf{0}$ implies that $\dot{\mathbf{x}}^\top \mathrm{D}\mathbf{p}\dot{\mathbf{x}} = 0$, it follows from Theorem 1 that $(\mathbf{x},\mathbf{y}) \in \mathcal{E}$ implies that $\dot{\mathbf{x}}^\top \mathrm{D}\mathbf{p}\dot{\mathbf{x}} = 0$. Furthermore, following the same analysis as in the proofs of [18, Theorem 7.2.9] or [30, Theorem 7.1], it is straightforward to show that $\mathbf{\Gamma}_P^\top \dot{\mathbf{x}} \le 0$ for all times, and that $\mathbf{\Gamma}_P^\top \dot{\mathbf{x}} = 0$ if and only if (8) holds. Consequently, we have that $\mathbf{\Gamma}_P^\top \dot{\mathbf{x}} + \dot{\mathbf{x}}^\top \mathrm{D}\mathbf{p}\dot{\mathbf{x}} \le 0$ for all times and that $\mathbf{\Gamma}_P^\top \dot{\mathbf{x}} + \dot{\mathbf{x}}^\top \mathrm{D}\mathbf{p}\dot{\mathbf{x}} = 0$ only when (8) holds. Now, let us consider the term $\mathbf{\Gamma}_G^\top \dot{\mathbf{y}}$. Observe that $\mathbf{\Gamma}_G^\top \dot{\mathbf{y}} = \sum_{q\in\mathcal{Q}} \dot{y}_{[q]} \int_0^{-g_{[q]}} [\sigma]_+ d\,\sigma$. Clearly, if $g_{[q]} \ge 0$, then $\int_0^{-g_{[q]}} [\sigma]_+ d\,\sigma = 0$. On the other hand, if $g_{[q]} < 0$, then $\int_0^{-g_{[q]}} [\sigma]_+ d\,\sigma > 0$ and $\dot{y}_{[q]} \le 0$ (the latter follows from (13) and the fact that $\mathbf{y} \in \mathbb{R}_{\ge 0}^{n_\mathcal{Q}}$ for all times). Hence, $\mathbf{\Gamma}_G^\top \dot{\mathbf{y}} \le 0$ for all times. In consequence, $\mathbf{\Gamma}_P^\top \dot{\mathbf{x}} + \dot{\mathbf{x}}^\top \mathrm{D}\mathbf{p}\dot{\mathbf{x}} + \mathbf{\Gamma}_G^\top \dot{\mathbf{y}} \le 0$ for all times, and, therefore, $\mathcal{E}$ is stable in the sense of Lyapunov.

To prove the asymptotic stability of $\mathcal{E}$, we rely on a LaSalle's Theorem [29, Theorem 3.3]. Namely, notice that $\mathbf{\Gamma}_G^\top \dot{\mathbf{y}} = 0$ if and only if it holds that

$$g_{[q]} < 0 \Rightarrow y_{[q]} g_{[q]} = 0, \quad \forall q \in \mathcal{Q}. \tag{15}$$

Hence, $\mathbf{\Gamma}_P^\top \dot{\mathbf{x}} + \dot{\mathbf{x}}^\top \mathrm{D}\mathbf{p}\dot{\mathbf{x}} + \mathbf{\Gamma}_G^\top \dot{\mathbf{y}} = 0$ if and only if $(\mathbf{x},\mathbf{y}) \in \mathcal{R}$, with $\mathcal{R} = \{(\mathbf{x},\mathbf{y}) \in \Delta \times \mathbb{R}_{\ge 0}^{n_\mathcal{Q}} : \text{(8) and (15) hold}\}$. Clearly, $\mathcal{E} \subseteq \mathcal{R}$. In fact, $\mathcal{E}$ is the subset of $\mathcal{R}$ where $g_{[q]} \le 0$ for all $q \in \mathcal{Q}$. Thus, if $\mathcal{E}$ is shown to be the largest invariant set of the dynamics within $\mathcal{R}$, then $\mathcal{E}$ is asymptotically stable under the considered dynamics (i.e., Lyapunov stable and attractive). We now proceed to prove such a property by contradiction.

Let $\mathcal{I} \subseteq \mathcal{R}$ be the largest invariant set of the dynamics within $\mathcal{R}$. Clearly, as $\mathcal{E} \subseteq \mathcal{R}$ is an invariant set (c.f., Theorem 1), it holds that $\mathcal{E} \subseteq \mathcal{I}$. Also, since $\mathcal{I}$ is an invariant set and $\mathcal{I} \subseteq \mathcal{R}$, it follows from Lemma 1 that $(\mathbf{x}(\tau),\mathbf{y}(\tau)) \in \mathcal{I} \Rightarrow \mathbf{x}(t) = \mathbf{x}(\tau)$, for all $t \ge \tau$. Now, suppose that $\mathcal{E} \subset \mathcal{I}$. That is, there exists some non-empty set $\mathcal{C} \subset \mathcal{I}$ such that $\mathcal{C} \cap \mathcal{E} = \emptyset$ and $\mathcal{C} \cup \mathcal{E} = \mathcal{I}$. Consequently, for every $(\mathbf{x}(\tau),\mathbf{y}(\tau)) \in \mathcal{C}$ it holds that: i) $\mathbf{x}(t) = \mathbf{x}(\tau)$ for all $t \ge \tau$ (because $\mathcal{C} \subset \mathcal{I}$); and ii) $\|\mathbf{y}(t)\| \to \infty$ as $t \to \infty$, where $\|\cdot\|$ is any p-norm (because there exists some $q \in \mathcal{Q}$ such that $g_{[q]}(\mathbf{x}(\tau)) > 0$, and thus $\dot{y}_{[q]}(\tau) = \dot{y}_{[q]}(t) > 0$, for all $t \ge \tau$). Hence, any $(\mathbf{x}(\tau),\mathbf{y}(\tau)) \in \mathcal{C}$ implies that the trajectories of the dynamics are unbounded for $t \ge \tau$. Clearly, this is a contradiction with the fact that $\mathcal{E}$ is stable in the sense of Lyapunov, and, therefore, we conclude that there cannot exist a non-empty set $\mathcal{C}$ such that $\mathcal{C} = \mathcal{I} \setminus \mathcal{E}$. In consequence, $\mathcal{I} = \mathcal{E}$, and $\mathcal{E}$ is asymptotically stable under the dynamics in (6)-(7). ■

REFERENCES

[1] J. Y. Yong, V. K. Ramachandaramurthy, K. M. Tan, and N. Mithulananthan, "A review on the state-of-the-art technologies of electric vehicle, its impacts and prospects," *Renewable and Sustainable Energy Reviews*, vol. 49, pp. 365–385, 2015.

[2] B. Li, M. C. Kisacikoglu, C. Liu, N. Singh, and M. Erol-Kantarci, "Big data analytics for electric vehicle integration in green smart cities," *IEEE Communications Magazine*, vol. 55, no. 11, pp. 19–25, 2017.

[3] Y. Yang, Q. Jia, G. Deconinck, X. Guan, Z. Qiu, and Z. Hu, "Distributed coordination of EV charging with renewable energy in a microgrid of buildings," *IEEE Transactions on Smart Grid*, vol. 9, no. 6, pp. 6253–6264, 2018.

[4] Y. Yang, Q. Jia, X. Guan, X. Zhang, Z. Qiu, and G. Deconinck, "Decentralized EV-based charging optimization with building integrated wind energy," *IEEE Transactions on Automation Science and Engineering*, vol. 16, no. 3, pp. 1002–1017, 2019.

[5] A. Ipakchi and F. Albuyeh, "Grid of the future," *IEEE Power and Energy Magazine*, vol. 7, no. 2, pp. 52–62, 2009.

[6] K. Clement-Nyns, E. Haesen, and J. Driesen, "The impact of charging plug-in hybrid electric vehicles on a residential distribution grid," *IEEE Transactions on Power Systems*, vol. 25, no. 1, pp. 371–380, 2010.

[7] M. S. ElNozahy and M. M. A. Salama, "A comprehensive study of the impacts of PHEVs on residential distribution networks," *IEEE Transactions on Sustainable Energy*, vol. 5, no. 1, pp. 332–342, 2014.

[8] N. I. Nimalsiri, C. P. Mediwaththe, E. L. Ratnam, M. Shaw, D. B. Smith, and S. K. Halgamuge, "A survey of algorithms for distributed charging control of electric vehicles in smart grid," *IEEE Transactions on Intelligent Transportation Systems*, vol. 21, no. 11, pp. 4497–4515, 2020.

[9] Z. Ma, S. Zou, and X. Liu, "A distributed charging coordination for large-scale plug-in electric vehicles considering battery degradation cost," *IEEE Transactions on Control Systems Technology*, vol. 23, no. 5, pp. 2044–2052, 2015.

[10] Z. Ma, S. Zou, L. Ran, X. Shi, and I. A. Hiskens, "Efficient decentralized coordination of large-scale plug-in electric vehicle charging," *Automatica*, vol. 69, pp. 35–47, 2016.

[11] S. Grammatico, "Exponentially convergent decentralized charging control for large populations of plug-in electric vehicles," in *Proceedings of the 55th IEEE Conference on Decision and Control (CDC)*, 2016, pp. 5775–5780.

[12] M. A. Tajeddini and H. Kebriaei, "A mean-field game method for decentralized charging coordination of a large population of plug-in electric vehicles," *IEEE Systems Journal*, vol. 13, no. 1, pp. 854–863, 2019.

[13] H. Ito, "Disturbance and delay robustness guarantees of gradient systems based on static noncooperative games with an application to feedback control for PEV charging load allocation," *IEEE Transactions on Control Systems Technology*, vol. 21, no. 4, pp. 1374–1385, 2013.

[14] H. Xing, M. Fu, Z. Lin, and Y. Mou, "Decentralized optimal scheduling for charging and discharging of plug-in electric vehicles in smart grids," *IEEE Transactions on Power Systems*, vol. 31, no. 5, pp. 4118–4127, 2016.

[15] Z. Ma, N. Yang, S. Zou, and Y. Shao, "Charging coordination of plug-in electric vehicles in distribution networks with capacity constrained feeder lines," *IEEE Transactions on Control Systems Technology*, vol. 26, no. 5, pp. 1917–1924, 2018.

[16] A. Ghavami, K. Kar, and A. Gupta, "Decentralized charging of plug-in electric vehicles with distribution feeder overload control," *IEEE Transactions on Automatic Control*, vol. 61, no. 11, pp. 3527–3532, 2016.

[17] G. Qu and N. Li, "On the exponential stability of primal-dual gradient dynamics," *IEEE Control Systems Letters*, vol. 3, no. 1, pp. 43–48, 2019.

[18] W. H. Sandholm, *Population games and evolutionary dynamics*. MIT Press, 2010.

[19] N. Quijano, C. Ocampo-Martinez, J. Barreiro-Gomez, G. Obando, A. Pantoja, and E. Mojica-Nava, "The role of population games and evolutionary dynamics in distributed control systems: The advantages of evolutionary game theory," *IEEE Control Systems Magazine*, vol. 37, no. 1, pp. 70–97, 2017.

[20] S. Park, N. C. Martins, and J. S. Shamma, "From population games to payoff dynamics models: A passivity-based approach," in *Proceedings of the 58th IEEE Conference on Decision and Control (CDC)*, 2019, pp. 6584–6601.

[21] J. Martinez-Piazuelo, N. Quijano, and C. Ocampo-Martinez, "A payoff dynamics model for equality-constrained population games," *IEEE Control Systems Letters*, vol. 6, pp. 530–535, 2022.

[22] D. Feijer and F. Paganini, "Stability of primal–dual gradient dynamics and applications to network optimization," *Automatica*, vol. 46, no. 12, pp. 1974–1981, 2010.

[23] C. Zhao, U. Topcu, N. Li, and S. Low, "Design and stability of load-side primary frequency control in power systems," *IEEE Transactions on Automatic Control*, vol. 59, no. 5, pp. 1177–1189, 2014.

[24] N. Li, C. Zhao, and L. Chen, "Connecting automatic generation control and economic dispatch from an optimization view," *IEEE Transactions on Control of Network Systems*, vol. 3, no. 3, pp. 254–264, 2016.

[25] J. Martinez-Piazuelo, N. Quijano, and C. Ocampo-Martinez, "Decentralized charging coordination of electric vehicles using multi-population games," in *Proceedings of the 59th IEEE Conference on Decision and Control (CDC)*, 2020, pp. 506–511.

[26] M. H. K. Tushar, A. W. Zeineddine, and C. Assi, "Demand-side management by regulating charging and discharging of the EV, ESS, and utilizing renewable energy," *IEEE Transactions on Industrial Informatics*, vol. 14, no. 1, pp. 117–126, 2018.

[27] M. C. Kisacikoglu, F. Erden, and N. Erdogan, "Distributed control of PEV charging based on energy demand forecast," *IEEE Transactions on Industrial Informatics*, vol. 14, no. 1, pp. 332–341, 2018.

[28] J. Forman, J. Stein, and H. Fathy, "Optimization of dynamic battery parameter characterization experiments via differential evolution," in *Proceedings of the 2013 American Control Conference*, 2013, pp. 867–874.

[29] W. M. Haddad and V. Chellaboina, *Nonlinear dynamical systems and control: a Lyapunov-based approach*. Princeton University Press, 2008.

[30] J. Hofbauer and W. H. Sandholm, "Stable games and their dynamics," *Journal of Economic Theory*, vol. 144, no. 4, pp. 1665–1693, 2009.